ELSEVIER

International Journal of Heat and Fluid Flow 22 (2001) 365–371

International Journal of HEAT AND FLUID FLOW

www.elsevier.com/locate/ijhff

# A statistical model for transport and deposition of high-inertia colliding particles in turbulent flow

L.I. Zaichik *, V.M. Alipchenkov

*Institute for High Temperatures, Russian Academy of Sciences, Krasnokazarmennaya 17a, 111250 Moscow, Russian Federation*

**Abstract**

The objective of the paper is to present a statistical model for predicting transport and deposition of high-inertia colliding particles in two-phase turbulent flows. This model is based on a kinetic equation for the probability density function (PDF) of the particle velocity distribution in a turbulent flow field. The model developed is applied to the simulation of fluctuating particle motion and deposition in vertical pipe flow. 

*Keywords:* Two-phase turbulent flow; Deposition; Inter-particle collisions; Vertical pipe

## 1. Introduction

When the volumetric fraction of the dispersed phase is small enough such that particle–particle collisions and fluid turbulence modulation are negligible, the particles move independently of one another. Therefore, in this case, the deposition flow rate on surrounding boundaries is proportional to the fraction of particles (drops), and the deposition coefficient is invariant with the particle fraction. In numerous experimental studies (e.g., Andreussi, 1983; Schadel et al., 1990; Hay et al., 1996), a distinct deviation of the deposition flow rate from a linear dependence and a pronounced decrease in the deposition coefficient were revealed as the particle fraction increases. The coalescence due to particle collisions is usually regarded to be responsible for this effect, causing the particle size to grow and the particle involvement in the fluctuating motion of a carrier turbulent flow to diminish. However, in Hay et al. (1996), it is noted that apparently the decrease in the deposition coefficient at large liquid flows cannot be explained solely by an increase in drop size. As an additional reason of reductions in the particle fluctuating velocity and the deposition coefficient with increasing particle fraction, a reduction in the eddy–particle interaction time that is directly attributed to particle encounters is considered. According to Hay et al. (1996), the eddy–particle interaction time is a function of collision frequency and, as result, is inversely proportional to the number of drops per unit volume, and thus authors explain the decrease in the deposition coefficient at large drop concentrations. At the same time, this conclusion seems to be contrary to the numerical results obtained by Laviéville et al. (1995) with the help of LES. As was found in Laviéville et al. (1995), elastic encounters do not virtually affect the particle fluctuating velocities and even slightly prolong the eddy–particle interaction time. Thus, the phenomenon of deposition of colliding particles in turbulent flow is not yet properly clarified.

An analytical model for predicting transport and deposition of high-inertia particles was developed by Zaichik (1998) and Zaichik et al. (1998). This model was based on second-moment equations and boundary conditions for particle velocities which had been derived from a kinetic equation for the probability density function (PDF) of particles in a dilute two-phase turbulent flow. The present paper describes further developments of the model in case of relatively large values of the particle volumetric fraction when particle–particle collisions must be allowed for.

## 2. Governing equations and boundary conditions

The velocities of two particles after a collision, $\boldsymbol{v}'_{\mathrm{p}}$ and $\boldsymbol{v}'_{\mathrm{p1}}$, are connected with their velocities before a collision, $\boldsymbol{v}_{\mathrm{p}}$ and $\boldsymbol{v}_{\mathrm{p1}}$, by the following relationships:

$$\boldsymbol{v}'_{\mathrm{p}} = \boldsymbol{v}_{\mathrm{p}} - \frac{1}{2}(1+e)(\boldsymbol{c}\cdot\boldsymbol{k})\boldsymbol{k}, \quad \boldsymbol{v}'_{\mathrm{p1}} = \boldsymbol{v}_{\mathrm{p1}} + \frac{1}{2}(1+e)(\boldsymbol{c}\cdot\boldsymbol{k})\boldsymbol{k}. \quad (1)$$

To derive a set of governing continuum equations and boundary conditions for predicting transport of the dispersed phase, we invoke a kinetic equation for the PDF of the particle velocity distribution. The statistical method based on kinetic transport equations for the PDF may be regarded as a consecutive approach to the creation of Eulerian two-fluid models for simulation of particle-laden turbulent flows. The introduction of the PDF permits to proceed from the dynamic stochastic description of separate particles to the statistical description of a particle ensemble as a whole. In this paper, a kinetic equation accounting simultaneously for both particle–turbulence interactions and particle–particle collisions is

* Corresponding author. Fax: 7-095-362-55-90.
*E-mail address:* zaichik@cityline.ru (L.I. Zaichik).

0142-727X/01/$ - see front matter 
PII: S 0 1 4 2 - 7 2 7 X ( 0 1 ) 0 0 1 0 0 - X

**Notation**

| | |
|---|---|
| $\boldsymbol{c}$ | relative velocity between two particles, $\boldsymbol{v}_p - \boldsymbol{v}_{p1}$ |
| $d_p$ | particle diameter |
| $e$ | restitution coefficient |
| $F_i$ | external force (e.g., gravity) acceleration |
| $g$ | acceleration due to gravity |
| $J_w$ | deposition flow rate |
| $j_+$ | particle deposition coefficient, $J_w/u_*\Phi$ |
| $\boldsymbol{k}$ | unit separation vector of two particles |
| $k_p$ | particle fluctuating kinetic energy, $\langle v'_k v'_k\rangle/2$ |
| $L$ | length macroscale of turbulence |
| $m$ | turbulence structure parameter |
| $P$ | probability density function |
| $P_2$ | particle–particle pair distribution function |
| $r$ | radial coordinate |
| $r_w$ | pipe radius |
| $R_D$ | mass deposition flow rate, $\rho_p J_w$ |
| $Re_p$ | particle Reynolds number, $\lvert\boldsymbol{W}\rvert d_p/\nu$ |
| $Sc_T$ | turbulent Schmidt number |
| $St$ | Stokes number |
| $T_E$ | Eulerian time macroscale of turbulence |
| $T_L$ | Lagrangian integral time-scale of turbulence |
| $T_{Lp}$ | eddy–particle interaction time |
| $t$ | time |
| $U_i$ | averaged velocity of the fluid (gas) |
| $u_0$ | turbulence intensity |
| $u_*$ | friction velocity |
| $\langle u'_i u'_j\rangle$ | fluid Reynolds stresses |
| $V_i$ | averaged velocity of the dispersed phase |
| $v_i$ | particle velocity |
| $\langle v'_i v'_j\rangle$ | particle kinetic stresses |
| $\boldsymbol{W}$ | averaged relative velocity between the fluid and a particle (drift velocity) |
| $x$ | streamwise (axial) coordinate |
| $x_i$ | Cartesian coordinates |
| $y$ | wall-normal coordinate |
| $Z$ | droplet mass concentration, $\rho_p\Phi$ |

*Greeks*

| | |
|---|---|
| $\gamma$ | drift parameter |
| $\nu$ | kinematic viscosity of the fluid |
| $\nu_T$ | turbulent viscosity coefficient |
| $\rho, \rho_p$ | densities of the continuous and dispersed phases |
| $\tau_p$ | particle relaxation time |
| $\tau_{p0}$ | Stokes relaxation time |
| $\tau_0$ | dimensionless particle relaxation time, $\tau_p u_*/r_w$ |
| $\tau_c, \tau_{c1}$ | characteristic intercollisional times |
| $\bar{\tau}_c$ | dimensionless intercollisional time |
| $\tau_*, \tau_{*1}$ | effective particle relaxation times |
| $\Phi$ | particle volumetric fraction |
| $\phi_x, \phi_y$ | restitution coefficients |
| $\Phi$ | particle volumetric fraction |
| $\chi$ | reflection coefficient |

employed. The turbulent velocity field of the carrier phase is modeled by a Gaussian random process, this enables the eddy–particle interaction in the kinetic equation to describe by a generalized Fokker–Plank differential operator (Derevich and Zaichik, 1988; Reeks, 1991). Thereafter, we restrict our consideration to not too dense particle clouds ($\Phi < 0.01$), when only double collisions are of importance, and the direct contributions of inter-particle encounters to stresses and fluxes are negligible. Moreover, inter-particle collisions are treated according to (1) by means of a hard-sphere model for pairs of mono-sized particles, as a result of which the collision term in the PDF equation is expressed in the form of a Boltzmann-type integral operator. In this way the PDF equation for high-inertia particles, the relaxation time of which is much longer than the eddy–particle interaction time ($\tau_p \gg T_{Lp}$), is given by

$$\frac{\partial P}{\partial t} + v_i\frac{\partial P}{\partial x_i} + \frac{\partial}{\partial v_i}\left(\frac{U_i - v_i}{\tau_p} + F_i\right) = \frac{T_{Lp}}{\tau_p^2}\langle u'_i u'_j\rangle\frac{\partial^2 P}{\partial v_i \partial v_j} + \frac{d_p^2}{4}\int\int P_2(\boldsymbol{v},\boldsymbol{v}_1)(\boldsymbol{c}\cdot\boldsymbol{k})\,d\boldsymbol{k}\,d\boldsymbol{v}_1. \quad (2)$$

Eq. (2) is valid for heavy particles, the density of which is much greater compared to that of the fluid and the size of which is smaller than the Kolmogorov length microscale. In this case, only the drag force acting on a moving particle by the surrounding fluid flow is of importance. The relaxation time,$\tau_p$, implies to be a function of the particle Reynolds number, and hence can account for the effect of interfacial drift velocity on the drag law. Here the particle relaxation time is determined by the relation

$$\tau_p = \frac{\tau_{p0}}{\varphi(Re_p)}, \quad \tau_{p0} = \frac{\rho_p d_p^2}{18\rho\nu},$$
$$\varphi(Re_p) = \begin{cases} 1 + 0.15Re_p^{0.687} & \text{for } Re_p \leqslant 10^3, \\ 0.11Re_p/6 & \text{for } Re_p > 10^3. \end{cases} \quad (3)$$

For closure of (2) it is required to presume the pair distribution function $P_2(\boldsymbol{v},\boldsymbol{v}_1)$. Fluctuating motion of two high-inertia particles can be regarded as an independent (uncorrelated) one. Therefore, similar to the kinetic theory of gases (i.e., to the so-called molecular chaos hypotheses), the particle–particle pair distribution function is defined as a product of the single-particle distribution functions, that is, $P_2(\boldsymbol{v},\boldsymbol{v}_1) = P(\boldsymbol{v})P(\boldsymbol{v}_1)$.

Eq. (2) generates a set of governing continuum equations representing the conservation of mass, momentum, particle turbulent stresses, and so on as the appropriate statistical moments of the velocity PDF. By this means the transport equations governing mass, momentum and kinetic stresses of the dispersed phase are written as

$$\frac{\partial\Phi}{\partial t} + \frac{\partial\Phi V_i}{\partial x_i} = 0, \quad (4)$$

$$\frac{\partial\Phi V_i}{\partial t} + \frac{\partial\Phi V_i V_j}{\partial x_j} = -\frac{\partial\Phi\langle v'_i v'_j\rangle}{\partial x_j} + \Phi\left(\frac{U_i - V_i}{\tau_p} + F_i\right), \quad (5)$$

$$\frac{\partial\Phi\langle v'_i v'_j\rangle}{\partial t} + \frac{\partial\Phi\langle v'_i v'_j\rangle V_k}{\partial x_k} = -\frac{\partial\Phi\langle v'_i v'_j v'_k\rangle}{\partial x_k} - \Phi\left(\langle v'_i v'_k\rangle\frac{\partial V_j}{\partial x_k} + \langle v'_j v'_k\rangle\frac{\partial V_i}{\partial x_k}\right) + \frac{2\Phi}{\tau_p}\left(\frac{T_{Lp}}{\tau_p}\langle u'_i u'_j\rangle - \langle v'_i v'_j\rangle\right) + J_{ij}, \quad (6)$$

$$\Phi = \int P\,d\boldsymbol{v}, \quad V_i = \frac{1}{\Phi}\int v_i P\,d\boldsymbol{v},$$
$$\langle v'_i v'_j\rangle = \frac{1}{\Phi}\int (v_i - V_i)(v_j - V_j)P\,d\boldsymbol{v}.$$

In (5), a collision term is absent because the total momentum of a particle system is conserved in the act of collisions. The collision term in (6) is rearranged by making use of familiar

Grad's method (Jenkins and Richman, 1985; Simonin, 1991; Zaichik and Pershukov, 1995)

$$J_{ij} = -\frac{2}{9}\left(1-e^2\right)\frac{k_p \Phi}{\tau_c}\delta_{ij} - \frac{2\Phi}{\tau_{c1}}\left(\langle v_i' v_j'\rangle - \frac{2}{3}k_p\delta_{ij}\right),$$
$$\tau_c = \left(\frac{2\pi}{3k_p}\right)^{1/2}\frac{d_p}{16\Phi}, \quad \tau_{c1} = \left(\frac{2\pi}{3k_p}\right)^{1/2}\frac{5d_p}{8(1+e)(3-e)\Phi}. \tag{7}$$

According to (7), the effect of particle–particle collisions on particle turbulent stresses consists of both the dissipation of fluctuating velocities due to inelastic impacts and the redistribution between different fluctuating velocity components (the return-to-isotropy term).

An equation for the third-order moments of particle velocity fluctuations is gained from (2) by using the assumption that the fourth-order cumulants are equal to zero, and hence the fourth-rank correlations are represented as sums of products of the second-order moments. The equation thus obtained is given by

$$\frac{\partial\langle v_i' v_j' v_k'\rangle}{\partial t} + V_n\frac{\partial\langle v_i' v_j' v_k'\rangle}{\partial x_n} + \langle v_i' v_j' v_n'\rangle\frac{\partial V_k}{\partial x_n} + \langle v_i' v_k' v_n'\rangle\frac{\partial V_j}{\partial x_n}$$
$$+ \langle v_j' v_k' v_n'\rangle\frac{\partial V_i}{\partial x_n} + \langle v_i' v_n'\rangle\frac{\partial\langle v_j' v_k'\rangle}{\partial x_n} + \langle v_j' v_k'\rangle\frac{\partial\langle v_i' v_k'\rangle}{\partial x_n}$$
$$+ \langle v_k' v_n'\rangle\frac{\partial\langle v_i' v_j'\rangle}{\partial x_n} + \frac{3}{\tau_p}\langle v_i' v_j' v_k'\rangle + J_{ijk} = 0. \tag{8}$$

In what follows the collision term in (8) is determined by means of 20-moments Grad's approximation

$$J_{ijk} = \frac{3}{\tau_{c1}}\left[\langle v_i' v_j' v_k'\rangle - E\left(\langle v_i' v_n' v_n'\rangle\delta_{jk} + \langle v_j' v_n' v_n'\rangle\delta_{ik} + \langle v_k' v_n' v_n'\rangle\delta_{ij}\right)\right],$$
$$E = \frac{1+3e}{18(3-e)} \tag{9}$$

The 13-moments Grad approximation yields the following expression for the convolutions of the third-rank correlations in (9)

$$\langle v_i' v_j' v_k'\rangle = \frac{1}{5}\left(\langle v_i' v_n' v_n'\rangle\delta_{jk} + \langle v_j' v_n' v_n'\rangle\delta_{ik} + \langle v_k' v_n' v_n'\rangle\delta_{ij}\right). \tag{10}$$

Eqs. (4)–(6) and (8) describe the mass and momentum transfer in the dispersed phase at the level of the third moments. To simulate the particle mass and momentum transfer at the level of the second-moment equations, it is necessary to derive algebraic relations for the third-rank correlations. These algebraic approximations can be obtain from (8) by neglecting time evolution, convection, and generation due to mean velocity gradients. As a result, with accounting for (9) and (10), the algebraic relations for the triple correlations are given by

$$\langle v_i' v_j' v_k'\rangle = -\frac{\tau_{*1}}{3}\left(\langle v_i' v_n'\rangle\frac{\partial\langle v_j' v_k'\rangle}{\partial x_n} + \langle v_j' v_n'\rangle\frac{\partial\langle v_i' v_k'\rangle}{\partial x_n} + \langle v_k' v_n'\rangle\frac{\partial\langle v_i' v_j'\rangle}{\partial x_n}\right),$$
$$\tau_{*1} = \frac{\tau_p \tau_{c1}}{\tau_{c1} + (1-5E)\tau_p}. \tag{11}$$

The form of (11) is consistent with the relations proposed by Hanjalić and Launder (1972) in turbulent single-phase flow, and by Wang et al. (1998) for the triple particle velocity correlations in dilute two-phase turbulent flow. As it is evident from (11), in moderately concentrated particulate two-phase flow ($\Phi < 0.01$), inter-particle collisions will cause the values of the triple velocity correlations to decrease, and thereby tend to diminish the diffusion transfer of particle velocity fluctuations. Conversely, in dense particle-laden flow ($\Phi \geqslant 0.1$), collisions will enhance the diffusion transfer through their direct contribution to the fluxes of fluctuating velocities (Zaichik and Pershukov, 1995).

To predict the particle transport and deposition we need knowledge of boundary conditions for governing equations (4)–(6). Relevant boundary conditions for dilute two-phase turbulent flow were defined by employing an approach based on solution of a kinetic PDF equation in the near-wall region by means of perturbation techniques (Derevich and Zaichik, 1988; Derevich, 1991; Zaichik, 1998). In such a manner, starting from (2), we obtain the following boundary conditions for the wall-parallel and wall-normal velocities and their fluctuations:

$$\left[V_y + \frac{1-\chi\phi_x}{1+\chi\phi_x}\left(\frac{2\langle v_y'^2\rangle}{\pi}\right)^{1/2}\right]V_x = \frac{\tau_*\langle v_y'^2\rangle}{2}\frac{dV_x}{dy}, \quad \tau_* = \frac{\tau_p\tau_{c1}}{\tau_p+\tau_{c1}}, \tag{12}$$

$$V_y = -\frac{1-\chi}{1+\chi}\left(\frac{2\langle v_y'^2\rangle}{\pi}\right)^{1/2}, \tag{13}$$

$$\left[V_y + \frac{1-\chi\phi_x^2}{1+\chi\phi_x^2}\left(\frac{2\langle v_y'^2\rangle}{\pi}\right)^{1/2}\right]\langle v_x'^2\rangle = \frac{\tau_{*1}\langle v_y'^2\rangle}{3}\frac{d\langle v_x'^2\rangle}{dy}, \tag{14}$$

$$V_y + \frac{1-\chi\phi_y^2}{1+\chi\phi_y^2}\left(\frac{8\langle v_y'^2\rangle}{\pi}\right)^{1/2} = \tau_{*1}\frac{d\langle v_y'^2\rangle}{dy}. \tag{15}$$

These boundary conditions take into consideration both the particle deposition and the effect of inelastic particle–wall collisions. In (12)–(15), the reflection coefficient, $\chi$, characterizes the deposition phenomenon and is equal to a probability of particle rebound from the wall and its return into the flow after a collision. The surface is perfectly absorbing if $\chi = 0$, and the particle deposition is absent if $\chi = 1$. The restitution coefficients, $\phi_x$ and $\phi_y$, allow for the momentum loss during the bouncing process, respectively, in the wall-parallel and wall-normal directions.

In the absence of inter-particle collisions, the above boundary conditions recover those obtained in Zaichik (1998). The influence of inter-particle collisions on the boundary conditions manifests itself in virtue of the diffusion transfer mechanism by substituting the effective relaxation time $\tau_*$ (or $\tau_{*1}$) for the particle relaxation time $\tau_p$.

Thus Eqs. (4)–(7), (11) and boundary conditions (12)–(15) enable one to describe the transport of colliding high-inertia particles in turbulent flow at the level of the second-order moments.

## 3. Eddy–particle interaction time

The Lagrangian fluid turbulence time-scale defined along a particle trajectory (the so-called eddy–particle interaction time) is a major quantity that characterizes the behavior of particles in turbulent flow. For very small (non-inertial) particles, the eddy–particle interaction time, $T_{Lp}$, coincides with the integral Lagrangian time-scale for a fluid point, $T_L$. However, for sufficiently inertial particles, $T_{Lp}$ can differ essentially from $T_L$, and, depending upon flow parameters, the ratio of $T_{Lp}/T_L$ may be both larger and smaller than unity. In this paper, $T_{Lp}$ is determined on the basis of the familiar Corrsin approximation for predicting relation between Lagrangian and Eulerian velocity correlation functions in isotropic turbulence. In this way we obtain the following relations for the eddy–particle interaction times according to the directions to be parallel and orthogonal to the drift velocity $\boldsymbol{W}$ (Zaichik and Alipchenkov, 1997)

$$T_{\mathrm{Lp}}^{\ell} = T_{\mathrm{E}} \int_0^{\infty} \left[ f(s) + \frac{s}{2} f'(s) - \left( m\gamma\tau + \frac{m\psi(\tau)}{\sqrt{3}} \right)^2 \frac{f'(s)}{2s} \right] \Psi_{\mathrm{E}}(\tau)\,\mathrm{d}\tau,$$

$$T_{\mathrm{Lp}}^{n} = T_{\mathrm{E}} \int_0^{\infty} \left[ f(s) + \frac{s}{2} f'(s) - \frac{m^2\psi^2(\tau)}{6s} f'(s) \right] \Psi_{\mathrm{E}}(\tau)\,\mathrm{d}\tau,$$

$$\psi(\tau) = \tau + St\left[\exp\left(-\frac{\tau}{St}\right) - 1\right] + St\left[\exp\left(-\frac{\tau - n\bar{\tau}_{\mathrm{c}}}{St}\right) - 1\right],$$

$$n\bar{\tau}_{\mathrm{c}} < \tau < (n+1)\bar{\tau}_{\mathrm{c}},\ n = 0,1,2,\ldots,$$

$$s = m\sqrt{\left[\gamma\tau + \frac{\psi(\tau)}{\sqrt{3}}\right]^2 + \frac{2\psi^2(\tau)}{3}},\quad St = \frac{\tau_{\mathrm{p}}}{T_{\mathrm{E}}},\quad \gamma = \frac{|\boldsymbol{W}|}{u_0},$$

$$\bar{\tau}_{\mathrm{c}} = \frac{\tau_{\mathrm{c}}}{T_{\mathrm{E}}},\quad m = \frac{u_0 T_{\mathrm{E}}}{L}. \qquad (16)$$

Here $\psi(\tau)$ stands for an effective run path of the particle in its fluctuating motion with accounting for the effect of inter-particle collisions. Referring to (16), $T_{\mathrm{Lp}}$ is controlled by at least four major factors, namely, the Stokes number $St$ characterizing the particle's response to fluid turbulence, the drift parameter $\gamma$ accounting for the so-called 'crossing-trajectories effect' (Yudine, 1959; Csanady, 1963), the dimensionless intercollisional time $\bar{\tau}_{\mathrm{c}}$, and the turbulence structure parameters $m$. In the case of no drift velocity ($\gamma = 0$) when the crossing-trajectories effect is absent, $T_{\mathrm{Lp}}$ raises with increasing $St$ and decreasing $\bar{\tau}_{\mathrm{c}}$ from $T_{\mathrm{L}}$ for small non-inertial particles to $T_{\mathrm{E}}$ for large heavy particles. The crossing-trajectories effect causes the eddy–particle interaction time to reduce as the drift parameter increases. Fig. 1 illustrates the influence of the drift parameter on $T_{\mathrm{Lp}}$ according to (16) for the frequent-used exponential and Gaussian correlation functions

$$f(s) = \Psi_{\mathrm{E}}(s) = \exp(-s) \quad \text{and} \quad f(s) = \Psi_{\mathrm{E}}(s) = \exp(-\pi s^2/4).$$

As seen, the results predicted are in reasonable agreement with LES computations of Deutsch and Simonin (1991).

## 4. Particle transport and deposition in vertical pipe flow

The model under development is applied to predicting transport and deposition of fairly massive droplets in a vertical, fully developed, round pipe flow. As suggested in a number of previous experimental and theoretical studies, the profiles of the averaged axial velocity and fluctuating velocities of large particles in pipes and channels are becoming relatively flat owing to intensive transverse mixing (i.e., these distributions in the pipe cross-section for massive particles are nearly uniform). Taking account of this fact, we can carry out a theoretical analysis for large particles ($\tau_{\mathrm{p}} \gg T_{\mathrm{Lp}}$) on the basis of asymptotic solution of governing equations (4)–(6) along with relationships (7), (11) and boundary conditions (12)–(15). In this approach, the profiles of the particle fraction, velocity and velocity fluctuations are found to be uniform, and their values are determined by appropriate mean characteristics of the carrier phase in the pipe cross-section considered.

By this means asymptotic solutions of Eqs. (4) and (5) with boundary conditions (12) and (13) are written as

$$V_x = \left(\bar{U}_x \mp \tau_{\mathrm{p}} g\right)\left[1 + \left(\frac{8}{\pi}\right)^{1/2}\left(\frac{1-\chi\phi_x}{1+\chi\phi_x} - \frac{1-\chi}{1+\chi}\right)\frac{\tau_{\mathrm{p}}\langle v_r'^2\rangle^{1/2}}{r_{\mathrm{w}}}\right]^{-1}, \qquad (17)$$

$$J_{\mathrm{w}} = \frac{4\Phi\tau_{\mathrm{p}}\langle v_r'^2\rangle}{r_{\mathrm{w}}}\left[1 + \left(\frac{1-\chi}{1+\chi}\left(\frac{2}{\pi}\right)^{1/2} + \frac{1+\chi}{1-\chi}4\left(\frac{\pi}{2}\right)^{1/2}\right) \times \frac{\tau_{\mathrm{p}}\langle v_r'^2\rangle^{1/2}}{r_{\mathrm{w}}}\right]^{-1}, \qquad (18)$$

where $V_x$ is the averaged particle velocity in the axial direction, and $J_{\mathrm{w}}$ is the particle flow rate on the wall in consequence of deposition. Here and afterwards, the overline symbolizes a mean quantity averaged with respect to the pipe cross-section, and the minus and plus signs in (17) refer to upward and downward flow, respectively.

In what follows, through the integration of (6) with accounting for (7), (11) and (14), (15) (the boundary condition for $\langle v_\varphi'^2\rangle$ is similar in form to $\langle v_x'^2\rangle$), the following set of algebraic equations for the axial, radial and tangential fluctuating mean square velocities is derived

$$\left(1+\frac{\tau_{\mathrm{p}}}{\tau_{\mathrm{c1}}}\right)\langle v_x'^2\rangle + \left(\frac{1-\chi\phi_x^2}{1+\chi\phi_x^2} - \frac{1-\chi}{1+\chi}\right)\left(\frac{2\langle v_r'^2\rangle}{\pi}\right)^{1/2}\frac{\langle v_x'^2\rangle\tau_{\mathrm{p}}}{r_{\mathrm{w}}} = \frac{\overline{T_{\mathrm{Lp}}\langle u_x'^2\rangle}}{\tau_{\mathrm{p}}} + \frac{2\tau_{\mathrm{p}}}{3\tau_{\mathrm{c1}}}Hk_{\mathrm{p}},$$

$$\left(1+\frac{\tau_{\mathrm{p}}}{\tau_{\mathrm{c1}}}\right)\langle v_r'^2\rangle + \frac{1-\chi\phi_y^2}{1+\chi\phi_y^2}\left(\frac{8\langle v_r'^2\rangle^3}{\pi}\right)^{1/2}\frac{\tau_{\mathrm{p}}}{r_{\mathrm{w}}} = \frac{\overline{T_{\mathrm{Lp}}\langle u_r'^2\rangle}}{\tau_{\mathrm{p}}} + \frac{2\tau_{\mathrm{p}}}{3\tau_{\mathrm{c1}}}Hk_{\mathrm{p}},$$

$$\left(1+\frac{\tau_{\mathrm{p}}}{\tau_{\mathrm{c1}}}\right)\langle v_\varphi'^2\rangle + \frac{1-\chi\phi_\varphi^2}{1+\chi\phi_\varphi^2}\left(\frac{2\langle v_r'^2\rangle}{\pi}\right)^{1/2}\frac{\langle v_\varphi'^2\rangle\tau_{\mathrm{p}}}{r_{\mathrm{w}}} = \frac{\overline{T_{\mathrm{Lp}}\langle u_\varphi'^2\rangle}}{\tau_u} + \frac{2\tau_{\mathrm{p}}}{3\tau_{\mathrm{c1}}}Hk_{\mathrm{p}},$$

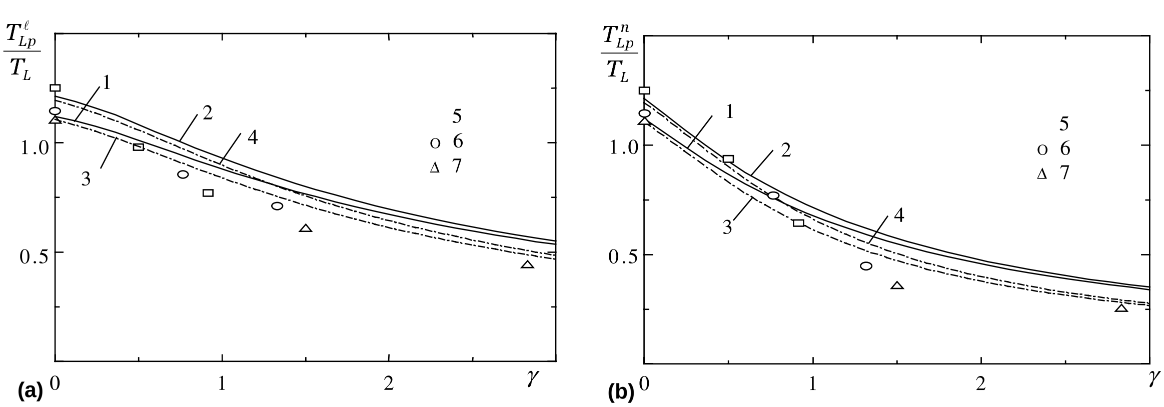


Fig. 1. Eddy–particle interaction times in the directions parallel (a) and orthogonal (b) to the mean relative velocity ($m = 1$): 1,2 – exponential correlations; 3,4 – Gaussian correlations; 1,3 – $St = 0.1$; 2,4 – $St = 0.2$; 5,6,7 – LES computations by Deutsch and Simonin (1991).

$$k_p = \frac{\langle v_x'^2\rangle + \langle v_r'^2\rangle + \langle v_\varphi'^2\rangle}{2}, \quad H = \frac{2(2+e)}{3(3-e)}. \tag{19}$$

It is apparent from (19) that, when the effect of inter-particle collisions does not play an important part ($\tau_p/\tau_{c1} \to 0$), the fluctuating velocity components are determined independently of one others, and hence, in order to calculate the deposition flow rate according to (18), one needs only find the particle radial velocity fluctuations $\langle v_r'^2\rangle$. In the case when the contribution of inter-particle collisions to the balance of particle stresses is of importance, to predict the deposition flow rate we need to resolve all the equations in (19).

Fluid turbulence characteristics in (19) are taken to be unchanged by the presence of particles. Furthermore, it is assumed that $\overline{T_{Lp}\langle u_r'^2\rangle} = \overline{T_L\langle u_r'^2\rangle}\bar{T}_{Lp}/\bar{T}_L$ and $\overline{T_L\langle u_r'^2\rangle} = \overline{\nu_T/Sc_T} = C_r u_* r_w$. Constant $C_r$ is taken to be of 5/81 (Zaichik et al., 1998) as a result of integrating well-known Reichardt's formula for the turbulent viscosity coefficient $\nu_T$ over the pipe cross-section when the turbulent Schmidt number is adopted as $Sc_T = 0.9$. The mean integral scales are defined as $\bar{T}_L = 0.08 r_w/u_*$, $\bar{T}_E = 0.2 r_w/u_*$, and $\bar{L} = 0.2 r_w$ (Zaichik et al., 1998). Moreover, according to experimental data for near-wall turbulent flows, the relations between various fluid fluctuating velocity components are taken as $\langle u_x'^2\rangle = 3\langle u_r'^2\rangle$ and $\langle u_\varphi'^2\rangle = 2\langle u_r'^2\rangle$.

Consider the deposition of particles on perfectly absorbing walls. In accordance with this assumption, the particle reflection coefficient, $\chi$, is taken to be zero. Then expression (17) for the averaged streamwise velocity of particles constricts to $V_x = (\bar{U}_x \mp \tau_p g)$, and, hence, because the particles absorbed on the wall do not return into the flow, one can exclude from consideration the effect of momentum loss by inelastic particle–wall collision. For $\chi = 0$, the deposition coefficient is determined according to (18) as

$$j_+ = \frac{4\tau_p\langle v_r'^2\rangle}{u_* r_w}\left(1 + \left(\sqrt{2/\pi} + \sqrt{8\pi}\right)\frac{\tau_p\langle v_r'^2\rangle^{1/2}}{r_w}\right)^{-1}, \quad C_1 = \left(\sqrt{2/\pi} + \sqrt{8\pi}\right)C_r^{1/2} = 1.44. \tag{20}$$

First we examine the deposition by neglecting the effect of inter-particle collisions ($\tau_p/\tau_{c1} \to 0$), when the particle radial velocity fluctuation intensity in (19) does depend on other fluctuating velocity components and is determined from the equation

$$\langle v_r'^2\rangle + \left(\frac{8\langle v_r'^2\rangle^3}{\pi}\right)^{1/2}\frac{\tau_p}{r_w} = \frac{\bar{T}_{Lp}}{\bar{T}_L}\frac{\overline{T_L\langle u_r'^2\rangle}}{\tau_p}. \tag{21}$$

Without accounting for both the influence of particle inertia and the crossing-trajectories effect on the eddy–particle interaction time, i.e., by taking $T_{Lp} = T_L$, from (20) and (21) it follows a simple approximation for the particle deposition coefficient (Zaichik, 1998)

$$j_+ = \frac{C_0(1 + C_2\tau_0^{1/3})^{-1}}{1 + C_1(1 + C_2\tau_0^{1/3})^{-1/2}\tau_0^{1/2}}, \quad C_0 = 4C_r = 0.247, \quad C_1 = \left(\sqrt{2/\pi} + \sqrt{8\pi}\right)C_r^{1/2} = 1.44, \quad C_2 = 2\left(\frac{C_r}{\pi}\right)^{1/3} = 0.54. \tag{22}$$

Figs. 2(a) and (b) show comparisons of predicted particle radial velocity fluctuations and deposition rates according to (20) and (21) with the results of DNS (Uijttewaal and Oliemans, 1996) in the absence of gravity. Curves 1 and 2 in these figures have been obtained, respectively, without and with accounting for the effect of particle inertia on the eddy–particle interaction time in accordance with (16), and so curve 1 in Fig. 2(b) corresponds to (22). As it is evident from the figures, taking this effect into consideration leads to a remarkably better coincidence with the DNS results. The decrease in the deposition coefficient as the particle inertia parameter $\tau_0$ increases is connected with a reduction in the response of particles to energy-containing turbulent velocity fluctuations of the carrier phase. Greater values of both parameters represented by curves 2 in comparison with curves 1 are caused by an increase in the eddy–particle interaction time when we take into consideration the effect of particle inertia on $T_{Lp}$, since the Eulerian time-scale is longer than the Lagrangian one. As a consequence of increasing $T_{Lp}$, the efficient particle inertia $\tau_p/T_{Lp}$, characterizing the involvement of particles in the turbulent motion of the fluid, diminishes, and hence the particles respond better to turbulent velocity fluctuations. This effect is similar in physical sense to the familiar phenomenon that the diffusivity of heavy particles can be more than the diffusivity of a passive scalar in the fluid that may also explain thereby $T_{Lp}$ is in excess of $T_L$ (e.g., Reeks, 1977; Wang and Stock, 1993).

Fig. 3 demonstrates the effect of particle–particle collisions on the particle fluctuating velocity components and the deposition coefficient predicted on the basis of (20) and (21) when the mean drift velocity is absent. Evidently the part of inter-particle collisions in particle fluctuating motion grows with decreasing intercollisional time, i.e., increasing $\tau_p/\tau_{c1}$. The influence of collisions on both the radial fluctuating velocity component and the deposition coefficient is revealed to depend radically on whether those are elastic or inelastic, therefore Fig. 3 presents results obtained for the limiting cases of totally inelastic ($e = 0$) and elastic ($e = 1$) particle–particle collisions. As it is obvious, elastic collisions, owing to the redistribution

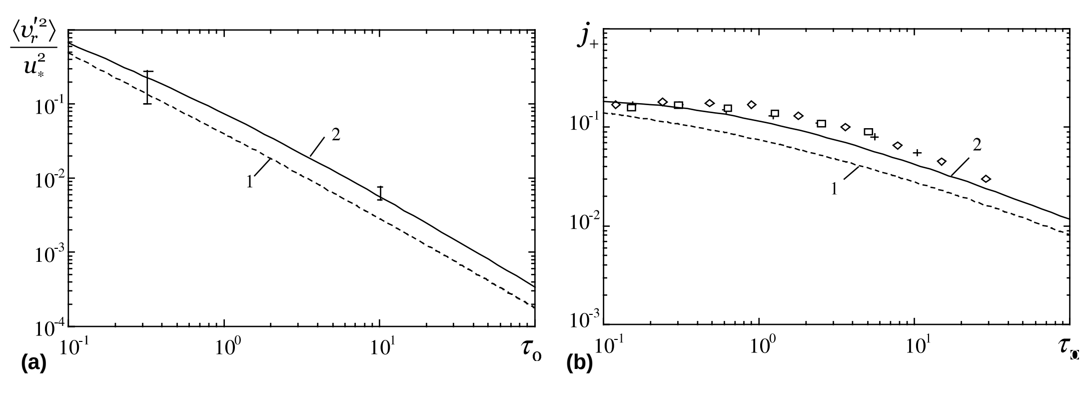


Fig. 2. Comparisons of predicted particle radial velocity fluctuations (a) and deposition rates (b) with the DNS results of Uijttewaal and Oliemans (1996) (symbols).

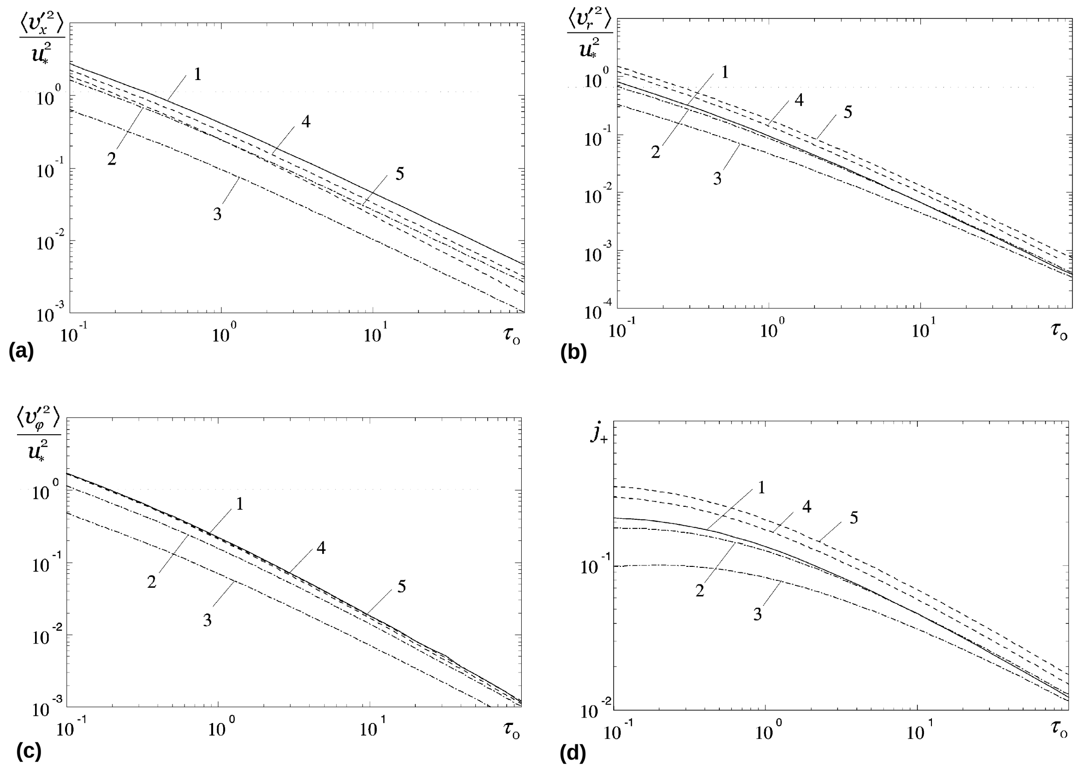


Fig. 3. Effect of inter-particle collisions on the axial (a), radial (b) and tangential (c) fluctuating velocity components as well as the deposition coefficient (d): 1 – $\tau_p/\tau_{c1} = 0$; 2,4 – $\tau_p/\tau_{c1} = 1$; 3,5 – $\tau_p/\tau_{c1} = 5$; 2,3 – $e = 0$; 4,5 – $e = 1$.

of turbulent energy between different velocity components, augment the wall-normal particle fluctuating velocities and increase consequently the deposition rate. Conversely, inelastic collisions can attenuate all the velocity fluctuation components and cause thereby a reduction in the particle deposition rate. This phenomenon is apparently typical for droplet-laden flows. However, a decrease in particle turbulence through inelastic particle–particle encounters, that was regarded as a major cause of a reduction in the deposition rate (Hay et al., 1996), is not of great importance for high-inertia particles ($\tau_0 \gg 1$).

In Fig. 4, the dependence of the mass deposition flow rate on the droplet mass concentration is displayed. The solid curve approximates experimental data (Hay et al., 1996), and the points represent calculations obtained using the mean diameters measured in Hay et al. (1996) for determining droplet relaxation times. Predictions have been carried out with allowing for impacts of inter-particle encounters on turbulence dissipation and redistribution according to (7) at $e = 0$, and also it takes into consideration influences of droplet inertia, interfacial drift and intercollisinal time on the eddy–particle interaction time. Fig. 4 displays a distinct deviation of $R_D(Z)$ from a straight line that is inherent in small-concentrated particle-laden systems. Calculations performed testify that the chief cases of the decrease in the deposition coefficient at large liquid flows are an increase in drop size due to coalescence and the crossing-trajectories effect. Immediate impacts of particle–particle collisions via turbulence dissipation and redistribution are not very important in the range of droplet concentration existing in experiments cited in Hay et al. (1996).

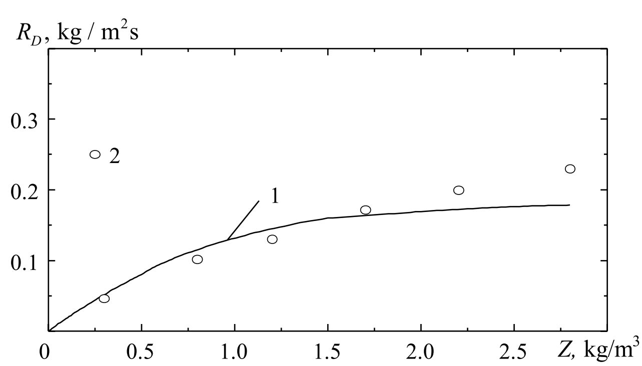


Fig. 4. The mass deposition flow rate against the droplet mass concentration: 1 – experimental approximation by Hay et al. (1996), 2 – predictions.

## 5. Summary

A statistical model for predicting transport and deposition of high-inertia colliding particles in turbulent flows is developed. This model is based on the kinetic equation for the PDF of the particle velocity distribution and takes simultaneously into consideration particle–turbulence interactions as well as inter-particle collisions. The model presented is employed for the simulation of fluctuating particle motion and deposition in vertical pipe flow.

On the basis of an analysis performed, the following conclusions can be drawn: (i) Elastic collisions increase the deposition rate, conversely inelastic collisions may result in a deposition decrease. (ii) The major cases of the reduction in the deposition coefficient at large liquid flows are an increase in drop size due to coalescence as well as the ‘crossing-trajectories effect’ due to gravity. (iii) In contrast, a decrease in particle turbulence through inelastic particle–particle collisions is not of great importance.

**Acknowledgements**

This work was supported by the Russian Foundation of Basic Investigations through grant 99-02-17001.

**References**

Andreussi, P., 1983. Droplet transfer in two-phase annual flow. Int. J. Multiphase Flow 9 (6), 697–713.

Csanady, G.T., 1963. Turbulent diffusion of heavy particles in the atmosphere. J. Atmos. Sci. 20, 201–208.

Derevich, I.V., 1991. The statistical concept of coarse particle motion in a turbulent pipe flow. In: Proceedings of the Eighth Symposium on Turbulent Shear Flows, Munich, Germany, pp. 1041–1046.

Derevich, I.V., Zaichik, L.I., 1988. Particle deposition from a turbulent flow. Fluid Dyn. 23 (5), 722–729.

Deutsch, E., Simonin, O., 1991. Large eddy simulation applied to the modelling of particulate transport coefficients in turbulent two-phase flows. In: Proceedings of the Eighth Symposium on Turbulent Shear Flows, Munich, Germany, pp. 1011–1016.

Hanjalić, K., Launder, B.E., 1972. A Reynolds stress model of turbulence and its application to thin shear flows. J. Fluid Mech. 52 (4), 609–638.

Hay, K.J., Liu, Z.-C., Hanratty, T.J., 1996. Relation of deposition to drop size when the rate law is nonlinear. Int. J. Multiphase Flow 22 (5), 829–848.

Jenkins, J.T., Richman, M.W., 1985. Grad's 13-moment system for a dense gas of inelastic spheres. Arch. Ration. Mech. Anal. 87, 355–377.

Laviéville, J., Deutsch, E., Simonin, O., 1995. Large eddy simulation of interaction between colliding particles and a homogeneous isotropic turbulence field. In: Proceedings of the Sixth International Symposium on Gas–Solid Flows, ASME FED 228, pp. 347–357.

Reeks, M.W., 1977. On the dispersion of small particles suspended in an isotropic turbulent fluid. J. Fluid Mech. 83 (3), 529–546.

Reeks, M.W., 1991. On a kinetic equation for the transport of particles in turbulent flows. Phys. Fluids A 3, 446–456.

Schadel, S.A., Leman, G.W., Binder, J.L., Hanratty, T.J., 1990. Rates of atomization and deposition in vertical annular flow. Int. J. Multiphase Flow 16 (3), 363–374.

Simonin, O., 1991. Second-moment prediction of dispersed phase turbulence in particle-laden flows. In: Proceedings of the Eighth Symposium on Turbulent Shear Flows, Munich, Germany, pp. 741–746.

Uijttewaal, W.S.J., Oliemans, R.V.A., 1996. Particle dispersion and deposition in direct numerical and large eddy simulations of vertical pipe flows. Phys. Fluids A 8 (10), 2590–2604.

Wang, L.P., Stock, D.E., 1993. Dispersion of heavy particles in turbulent motion. J. Atmos. Sci. 50 (13), 1897–1913.

Wang, Q., Squires, K.D., Simonin, O., 1998. Large eddy simulation of turbulent gas–solid flows in a vertical channel and evaluation of second-order models. Int. J. Heat Fluid Flow 19, 505–511.

Yudine, M.I., 1959. Physical consideration on heavy-particle dispersion. Adv. Geophys. 6, 185–191.

Zaichik, L.I., 1998. Transport and deposition of inertial particles in turbulent pipe flow. ERCOFTAC Bull. 36, 16–19.

Zaichik, L.I., Alipchenkov, V.M., 1997. Simulation of transport of colliding particles suspended in turbulent shear flows. In: Proceedings of the Second International Symposium on Turbulence, Heat and Mass Transfer, Delft, The Netherlands, pp. 823–831.

Zaichik, L.I., Nigmatulin, B.I., Alipchenkov, V.M., 1998. Droplet deposition and film atomization in gas–liquid annular flow. In: Proceedings of the Third International Conference on Multiphase Flow, Lyon, France.

Zaichik, L.I., Pershukov, V.A., 1995. Modeling of particle motion in a turbulent flow with allowance for collisions. Fluid Dyn. 30 (1), 49–63.